University of Arkansas, Fayetteville
ScholarWorks@UARK

Theses and Dissertations

8-2017

Evaluating Methods for Quantifying Evapotranspiration in Arkansas Rice

Colby Reavis
University of Arkansas, Fayetteville

Follow this and additional works at: http://scholarworks.uark.edu/etd

 Part of the Agronomy and Crop Sciences Commons, and the Bioresource and Agricultural Engineering Commons

Recommended Citation
Reavis, Colby, "Evaluating Methods for Quantifying Evapotranspiration in Arkansas Rice" (2017). *Theses and Dissertations*. 2493.
http://scholarworks.uark.edu/etd/2493

This Thesis is brought to you for free and open access by ScholarWorks@UARK. It has been accepted for inclusion in Theses and Dissertations by an authorized administrator of ScholarWorks@UARK. For more information, please contact ccmiddle@uark.edu, drowens@uark.edu, scholar@uark.edu.

Evaluating Methods for Quantifying Evapotranspiration in Arkansas Rice

A thesis submitted in partial fulfillment
of the requirements for the degree of
Master of Science in Biological Engineering

by

Colby Wade Reavis
University of Arkansas
Bachelor of Science in Biological Engineering, 2014

August 2017
University of Arkansas

This thesis is approved for recommendation to the Graduate Council

_____
Dr. Benjamin R.K. Runkle
Thesis Director

_____
Dr. Brian E. Haggard
Committee Member

_____
Dr. Michele L. Reba
Committee Member

Abstract

The goal of this study was to evaluate different methods for quantifying evapotranspiration (ET) in commercial rice fields using different irrigation regimes. The rice fields were located in south central Arkansas. The different irrigation regimes were alternate wetting and drying (AWD) and continuous flooding (CF). Alternate wetting and drying and conventional flooding estimates of ET were 602 mm and 570 mm, respectively, based on field observations using eddy covariance. Models used to estimate ET estimated values between 498 and 653 mm for the 2015 growing season. The Penman Monteith actual evapotranspiration model (PM AET) performed best when compared to the eddy covariance field observations from both irrigation regimes using an iteration of the Jarvis model for conductance, which was scaled using field observations of leaf area index (LAI). The Breathing Earth Systems Simulator (BESS), a global product based on remote sensing data, also served as an acceptable method to estimate ET, though its estimated ET of 498 mm indicates a low bias. AWD showed no significant reductions in ET when compared to CF throughout the growing season, including during periods where the AWD field was confirmed to have a water table depth below zero. This pattern was also consistent in observing the PM AET model over the same periods of time. The lack of changed ET rates while the water table was fluctuating implies that while the water table was below zero, the rice plants within the AWD field did not experience significant drought stress. Because the AWD plants retained a normal amount of stomatal activity and production, there were also no significant differences in yield (9.42 ± 0.82 t ha^{-1} in CF, 9.83 ± 1.02 t ha^{-1} in AWD). These results indicate that AWD did not induce drought stress within the plants while still being able to take advantage of seasonal rain fall to offset pumping costs.

Acknowledgements

I would like to first thank my wife, Megan, and my family for their support during this time. I owe an immense amount of gratitude to my advisor, Dr. Benjamin Runkle, for allowing me to participate in this project while also investing in me and encouraging me to be a better thinker, researcher, communicator, and team mate. I would also like to thank my committee members, Drs. Michele Reba and Brian Haggard, for their guidance and commitment to help this project succeed. This work would not have been possible without Dr. Kosana Suvocarev, who provided a great wealth of information and guidance while also working nonstop to ensure our group stays afloat. Thank you to the Isbell family for allowing our lab group to have full access to their rice fields and being exceedingly accommodating throughout our time together. Special thanks to Bryant Fong and Jack Chiu for their assistance and recommendations in the field. Thanks to Faye Smith for her help in data acquisition.

Table of Contents

Introduction

Arkansas produces 50% of the rice within the U.S., and the rice industry provides benefits to the state economically, accounting for 25,000 jobs and greater than $2 billion in revenue generated for the state (AR Rice, 2011). Rice production is water intensive when grown using continuous flood irrigation practices, which utilize continuous inundation to provide water for the crop and help prevent the growth of weeds. The generated flood is typically held for a majority of the growing season (May – late August) and can be supplied by groundwater or nearby surface water. The flood is typically applied once the rice plant achieves the desired stage and drained before harvest. The rice is allowed two weeks to dry after drainage before harvest.

Conventionally managed rice can also require over 9 million liters of water per ha (Anders et al., 2012). Currently, water resources are being consumed at unsustainable rates within the Mississippi Delta region of Arkansas where rice is grown (Reba et al., 2013). Depletion rates amount to 8036 million gallons per day for the alluvial aquifer water supply and 159 million gallons per day for the Sparta/Memphis aquifer (ANRC, 2015). Due to this depletion, the state of Arkansas is increasing efforts to conserve water and quantify water usage, particularly within agricultural irrigation (ANRC, 2014).

To promote conservation of water within rice production, a number of methods and approaches are being applied, such as zero-grade leveling, which has been shown to reduce irrigation water use by up to 40% (Henry et al., 2016). One irrigation practice that has potential for water savings is Alternate Wetting and Drying (AWD). The AWD practice, unlike the continuous flood irrigation practice, allows periodic drying to occur once the plant has reached a specific stage of development. Ideally, in a controlled environment, the soil would be allowed to reach a specified moisture content during dry down, and then the flood would be reapplied.

AWD conserves water by taking advantage of rains during the growing season to offset pumping costs for the producer, sometimes reducing water use by up to 20% (Linquist et al., 2015; Carrijo et al., 2017; Pan et al., 2017; Lampayan et al., 2015). The level of drying that occurs is largely subjective and often depends on multiple factors, including infrastructure, plant variety, and water supply.

To evaluate the potential water savings associated with AWD, uncertainty must be reduced around terms within the rice system water balance. The basic water balance for rice includes irrigation water applied, precipitation, infiltration, runoff, drainage, and evapotranspiration. One of the key terms within this system is evapotranspiration (ET), consisting of evaporation and plant transpiration. Quantifying ET has the benefit of reflecting changes in above-ground water table. With the declining water table depth in AWD, the evaporation portion of ET should decrease as less water becomes available for evaporation.

ET has been estimated a number of ways in the past, using a variety of instrumental, meteorological, and modeling approaches. In agriculture, ET instruments such as evaporation pans and atmometers have been used to estimate reference evapotranspiration (Allen & Pruitt, 1991; Lamine et al., 2015). Other approaches involve the use of meteorological and biometeorological data to model actual or potential ET in the system, such as the Penman-Monteith or Priestley-Taylor methods (Penman, 1948; Priestley & Taylor, 1972; Monteith, 1981). Other approaches, such as eddy covariance, use advanced micrometeorological instrumentation to find the covariance between high frequency measurements of gas concentrations and high frequency vertical wind movements, which provides a calculated land-atmosphere flux of a selected gas (Baldocchi et al., 1996; Timm et al., 2014).

1. **Problem Definition**

1.1 Study Objectives

The goal of the current study is to provide an estimate of ET for rice fields using different irrigation regimes and begin establishing the grounds for a full water balance within a rice growing system. We examine how ET varies between fields using continuous flood and AWD irrigation practices, and we also investigate possible drivers for these differences. For this experiment, ET will be estimated using the following methods (to be described later):

- Eddy covariance (EC)
- Penman-Monteith classical method (PM AET)
- Penman-Monteith method as outlined in FAO Drainage Paper 56 (PM FAO56)
- Priestley-Taylor method (PT)
- Breathing Earth System Simulator (BESS)

While the other methods utilize meteorological and biometeorological data to estimate ET, eddy covariance directly measures water vapor concentrations to estimate ET, making it distinctly different and suitable as an observational data set. We plan to reduce uncertainty associated with ET in the field sites by (1) establishing an estimate of ET from each model and field observations, (2) evaluate how models perform across different temporal scales and field conditions, (3) observe driving forces of ET within each model, and (4) correlate physiological development of the rice crop to different variables to improve model performance.

1.2 Hypotheses

This study addresses three hypotheses, with H(O) representing the null hypothesis and H(A) representing the alternative.

H(O)1: Alternate wetting and drying allows for a decrease in the evaporation portion of ET due to the decreasing amount of water above the ground.

H(A)1: AWD and CF had no significant differences in ET, likely due to the ratio of transpiration to evaporation, dissimilar planting densities, and the plant's ability to still access water in the root zone.

H(0)2: The model with the highest number of explanatory input variables will produce the best estimate of ET.

H(A)2: Model complexity did improve performance, but the number of inputs was not as important as ensuring the model accounted for both the meteorological and physiological aspects of the rice canopy.

H(0)3: Models utilizing the daily time scale will produce estimates of ET that are similar to models operating at the sub-daily time scale.

H(A)3: Models using different time steps for data provided comparable seasonal estimates of ET.

2. Materials and Methods

2.1. Site Description

The study site for this experiment is composed of two adjacent fields located in eastern Arkansas, USA near the village of Humnoke (34° 35' 8.58" N, 91° 44' 51.07" W). The fields are commercial scale (~24 ha each), and have been used to grow rice in continuous rotation. The fields are zero-graded with no slope within the area of the field. The soil within the fields is primarily characterized by poorly-draining clays mixed within a variety of soil types.

Rice grown within the fields is a hybrid variety (Clearfield XL745), and the typical growing season for rice in Arkansas extends from early April to September. Irrigation during the growing season relies on pumped surface water, which travels between fields using pipes and force of gravity. During the 2015 growing season, one field received alternate wetting and drying treatment while the other field received conventional flooding.

Equipment within the fields, including instruments, were installed directly after planting, and instruments were only removed for harvest and maintenance. The instrumentation consisted of key eddy covariance components as well as a number of biometeorological sensors. Based on the requirements for the eddy covariance technique, the equipment was installed at the northern border of each field to capture the dominant southern winds during the growing season.

2.2. Measurement of fluxes, microclimate, and plant parameters

The eddy covariance (EC) system provided measurements of sensible heat (H) and latent heat (LE flux). The EC system included a 3D sonic anemometer (CSAT3, Campbell Scientific, Inc., USA), an open-path infrared CO_2/H_2O analyzer (LI-7500, LI-COR, Inc., Lincoln, NE, USA), and an open-path CH_4 analyzer (LI-7700, LI-COR, Inc., Lincoln, NE, USA). The EC system was mounted on a tripod, with the sensor height measuring 2.5 m above the surface of the rice field. Separation for the EC sensors was approximately 0.1 m and accounted for with frequency correction factors and signal lagging. For logging, the EC components used a designated analyzer interface unit (LI-7550, LI-COR, Inc., Lincoln, NE, USA). The unit recorded EC sensor outputs at 20 Hz and fluxes were calculated with Eddy Pro v. 6.2 software. Measured fluxes received quality control treatment based on turbulence and wind direction. Fluxes at the 30-min time scale underwent gap filling using artificial neural networks (Papale & Valentini., 2003). Net radiation was measured in 4-components (CNR4, Kipp & Zonen, Inc.,

Netherlands, EUR) at a height of 2 m. Photosynthetically active radiation (PAR) was also measured using quantum sensors (LI-190SB, LI-COR, Inc., Lincoln, NE, USA) at 1.85 m. Soil heat flux measurements were collected using soil heat flux plates (HFP01, Hukseflux, Netherlands, EUR). Soil surface temperature and water temperature were measured using thermistors (CS-107 (BetaTherm 100K6A1IA), Campbell Scientific, Inc., USA). Air temperature and relative humidity were measured using a shielded probe (HMP155A, Vaisala, Finland, EUR). Volumetric water content measurements were collected using soil moisture probes (SDI-12, Acclima, Sydney, AU). Water depth measurements were collected continuously using a piezometric sensor (Series 46x, Keller, USA). Other field parameters including plant density and bulk soil density were collected manually at different times during the growing season as well.

2.3 Crop height and LAI model

Plant height measurements were collected throughout the growing season, using a 10-measurement average during each excursion. Leaf area index (LAI) was also measured in a similar manner using a handheld device (LI-2200, LI-COR, Inc., Lincoln, NE, USA). Estimating LAI and plant height throughout the growing season required the development of a growing-degree-day (GDD) model (Yang et al., 1995). The growing degree day is a function of mean daily temperature and a base temperature, often selected as the minimum temperature for development to occur within a specific type of vegetation or crop (Equation 1).

$$GDD = \frac{(T_{mean,daily})}{2} - T_{base} \qquad \text{(Equation 1)}$$

Where $T_{mean,daily}$ represents the mean daily temperature and T_{base} represents the minimum temperature required for plant development (12ºC for rice). A GDD value is calculated each day

of the growing season, with a total GDD value accumulating over time. In instances where the mean daily temperature was less than or equal to T_{base}, the calculated GDD was set to zero.

2.4 Evapotranspiration modeling methods

During the 2015 growing season, four key methods were used for estimating ET within the continuously flooded and alternate-wetting-and-drying fields. Each method was compared to eddy covariance observations, which provided direct measurements of ET for each field. Eddy covariance is a technique that uses the analysis of micrometeorological data to determine the fluxes occurring between the ground and atmosphere. The method observes the covariance between measured gas concentrations and changing 3D wind speeds to generate estimates of flux for different gases, including water vapor (Baldocchi et al., 1996). The eddy covariance method has the advantage of measuring at high frequencies and collecting a large, continuous data set while the equipment is deployed within the field. It should be stated that although eddy covariance provides direct measurements, it also has the potential to underestimate fluxes, including latent heat exchange (Foken et al., 2006).

Providing a diverse set of approaches will ideally limit the uncertainty of ET within each field while also showing how each method compares across different time and spatial scales. For this reason, the 4 elected methods differ in complexity and approach as well as spatial and temporal resolution. The methods include the PM AET approach, the PM FAO 56 approach, the Priestley-Taylor approach, and the Breathing Earth System Simulator based on remote sensing datasets. The methods are defined below:

1. **The Penman-Monteith for Actual ET (AET) (PM AET)**. This modeling method develops an estimate for actual evapotranspiration (AET) based on meteorological data and information about plant development within the system. The combination equation

(Equation 2) is based around the energy requirement to cause vaporization as well as the deficit of water necessary for removing vapor (Penman, 1948; Monteith, 1965). It will be used to evaluate data collected in real time from both fields at the 30-min time step.

$$\boldsymbol{\lambda ET} = \frac{\boldsymbol{\Delta(R_n - G) + c_p p_a \frac{(e_s - e_a)}{r_a}}}{\boldsymbol{\Delta + \gamma\left(1 + \frac{r_s}{r_a}\right)}} \qquad \text{(Equation 2)}$$

Where,

- λET latent heat flux, W m^{-2}
- R_n net radiation, W m^{-2}
- G soil heat flux, W m^{-2}
    - Estimated ground heat flux *G* using ratio of *G* to net radiation, R_n as outlined in FAO-56
- c_p specific heat of air, J kg^{-1} °C^{-1}
- p_a mean air density, kg m^{-3}
- $e_s - e_a$ vapor pressure deficit, kPa
- r_s bulk surface resistance, s m^{-1}
- r_a aerodynamic resistance, s m^{-1}
- Δ slope of vapor pressure-temperature relationship, kPa °C^{-1}
- γ psychrometric constant, kPa °C^{-1}

2. **Revised Penman Monteith FAO-56 Model (PM FAO56).** Based on the work of Howard Penman, this modeling method generates an estimate of actual evapotranspiration that is based on meteorological variables as well as canopy characteristics within agricultural settings (Allen et al., 1998). The FAO-56 method (Equation 3) generates daily estimates of AET, and the estimated ET (mm day^{-1}) is calculated using crop coefficients unique to the different developmental stages of a specific crop. For this method, several assumptions were made in relation to the reference

evapotranspiration and ground heat flux. Reference evapotranspiration requires measurements taken from a representative plot that adheres to FAO 56 standards so that all other assumptions inherent to the model hold. For this experiment, the measurements were instead taken directly from at the observed rice field as there was no suitable FAO-56 reference grass or alfalfa site in the nearby area. Net radiation was estimated using "missing climate data methods" outlined in FAO 56 based on the location of the site as well as the day of year and daily ground heat flux *G* is assumed by FAO 56 to be a fraction of net radiation during the day (10%) and night (40%). Temperature, relative humidity, and wind speed measurements at the rice field were assumed to be representative of conditions surrounding an FAO 56 plot.

$$\boldsymbol{ET = ET_0 * K_c = \frac{0.408\Delta(R_n - G) + \gamma\left(\frac{C_n}{T+273}\right)(e_s - e_a)u_{2m}}{\Delta + \gamma(1 + C_d u_{2m})} * K_c} \qquad \text{(Equation 3)}$$

Where,

- ET evapotranspiration, mm day^{-1}
- R_n net radiation, MJ m^{-2} day^{-1}
- G soil heat flux, MJ m^{-2} day^{-1}
- $e_s - e_a$ vapor pressure deficit, kPa
- Δ slope of vapor pressure curve, kPa °C^{-1}
- γ psychrometric constant, kPa °C^{-1}
- T mean daily air temperature at 2m height, °C
- u_{2m} wind speed at 2 m height, m s^{-1}
- C_d,C_n coefficients based on canopy development for tall alfalfa crop
- K_c crop coefficient for converting reference ET to ET of study crop

3. **Priestley-Taylor (PT).** The Priestley-Taylor method (Equation 4) provides the simplest approach to estimating actual evapotranspiration (AET) within our field site. The method

relies on measurements of available energy, temperature, and relative humidity. This method requires no input for specific crop characteristics or other landscape parameters. The Priestley-Taylor equation does utilize a coefficient, α, which represents the ratio of equilibrium ET to actual ET and historically valued at 1.26 (Stewart & Rouse, 1977).

$$\boldsymbol{ET = ET_{eq} * \ \alpha} = \frac{\Delta}{\Delta + \boldsymbol{\gamma}} * (R_n - G) * \alpha \qquad \text{(Equation 4)}$$

Where,

- Δ slope of vapor pressure curve, kPa °C^{-1}
- γ psychrometric constant, kPa °C^{-1}
- R_n net radiation, MJ m^{-2} day^{-1}
- G soil heat flux, MJ m^{-2} day^{-1}
- α Priestley-Taylor coefficient,

4. **Breathing Earth Systems Simulator (BESS).** The BESS is a remote sensing approach for measuring ET and gross primary production (GPP) for multiple landscapes, including rice (Jiang & Ryu, 2016). BESS generates ET estimates across fine spatial scales (<1 km^2), including for the previous decade using legacy data. BESS is advantageous in that it requires very little input information from the user while still being able to derive accurate estimates of ET using a number of global databases, including MODIS products created to derive information from the landscape and surrounding atmosphere. This allows the user to observe larger spatial areas for trends while ensuring the integrity of the model is sound and consistent.

Three of the methods (Priestley-Taylor, PM AET, and PM FAO56) rely on direct measurements of variables from the field site, which are then used to calculate ET separately from the eddy covariance operations (Table 1).

Table 1. Summary of outputs and time scales of key terms for actual evapotranspiration (AET) methods utilizing instrumental measurements

Method	Output	T	R_n	RH	Wind speed	Others
Priestley-Taylor	AET	Mean daily	Mean daily	Mean daily	-	Calibration coefficient (α)
PM AET	AET	Mean 30-min	Mean 30-min	Mean 30-min	Mean 30-min	LAI, plant height, surface conductance (g_c)
PM FAO56	AET	Mean daily	Mean daily	Mean daily	Mean daily	Crop coefficient (K_c)

For the half-hourly (30-min) time scale, direct measurements were used with a sampling frequency of 20 Hz. Daily estimates of variables were calculated from the 30-min data collected over the growing season.

2.5 Modeling approach and evaluation metrics

The models will first be used to establish a baseline amount of evapotranspiration from the conventionally flooded field. Understanding how each model behaves when irrigation is not limited will benefit any future comparisons by identifying key meteorological and biological drivers that should be similar across other regional fields, the majority of which are conventionally flooded. The models will then be applied to the AWD field to see if the changing water table can be linked to changes in key drivers within each model. Water table data will be

coupled to observational periods of eddy covariance ET data to classify periods of "wet" and "dry" between the AWD and CF fields. The "wet" classification represents periods where the water table in both fields is above the surface of the soil. The "dry" classification represents periods where the CF water table is above the surface of the soil while the AWD water table is below the surface of the soil. This process should reveal how water table affects ET across periods where canopy development is similar between the two fields.

To reduce uncertainty surrounding ET associated with each irrigation regime, ET estimates were compared across multiple temporal scales, including half-hourly and daily periods. Key indicators of model performance were coefficient of determination (R^2) and root mean square error (RMSE). While eddy covariance measurements were used as the observational dataset upon which to test model performance, models were also compared to one another to identify a potential consensus.

Another goal of this research is to model conductance as an input to the PM AET equation to improve model performance in both fields. Models for conductance were selected from literature and calibrated using data collected from each field. Performance was based on how well the modeled conductance output improved the PM AET equation when estimation ET via R^2 and RMSE. Conductance models were selected individually based on performance within each irrigation regime and applied to the PM AET model for further comparison.

2.6 Modeling crop coefficients

A crop coefficient was necessary to estimate actual evapotranspiration using the PM FAO56 method. Crop coefficient values have been given in the FAO 56 document for rice grown in different areas of the world (Doorenbros & Kassam, 1979; Doorenbros & Pruitt, 1977; Snyder, Shaw & Pruitt, 1989a). To improve the method, a localized crop coefficient was

estimated using field observations (Equation 5) and calculated reference ET (based on field measurements, not an FAO 56 standardized plot).

$$K_{c,local} = \frac{ET_{observed}}{ET_{reference}} \quad \text{(Equation 5)}$$

The estimated crop coefficient provided evidence linking plant development terms not present within the model to the developing crop coefficient. Comparisons were made between the development of the plant via measurements of plant height and LAI to the estimated local crop coefficient. Because the previously mentioned terms are independent of the PM FAO56 method, integrating them through the crop coefficient term could improve the estimation of ET as well.

2.7 Modeling canopy conductance

Canopy conductance is a key term within the PM AET model which reflects biological mediation of the exchange of gases between the rice canopy and the surrounding atmosphere. To gain an estimate of canopy conductance within each field site, the PM AET model was first inverted to solve for canopy conductance, g_c (Equation 6).

$$\frac{1}{g_c} = \boldsymbol{r_s} = \left(\left(\frac{\left(\left(\frac{\boldsymbol{\Delta}(\boldsymbol{R_n} - \boldsymbol{G}) + \boldsymbol{c_p p_a} \frac{(\boldsymbol{e_s} - \boldsymbol{e_a})}{\boldsymbol{r_a}}}{\boldsymbol{\lambda ET_{eddy\ covariance}}} \right) - \boldsymbol{\Delta} \right)}{\boldsymbol{\gamma}} \right) - 1 \right) * \boldsymbol{r_a} \quad \text{(Equation 6)}$$

During inversion, eddy covariance observations were used for the evapotranspiration term, but data from the gap filling procedure using artificial neural networks were removed. The calculated observed estimate of surface conductance is used in conjunction with terms linked to conductance (vapor pressure deficit, photosynthetically active radiation, etc.) to create a model which provides estimates of conductance based on the changing biometeorological conditions of the canopy throughout the growing season.

The models applied to estimated canopy conductance varied in complexity and development, and were evaluated based on how well the modeled conductance fit the calculated conductance values. Each time series of modelled conductance was applied to the PM AET model, and the estimates of ET coming from the PMAET model were compared to one another. The methods for estimating conductance were multiple linear regression (MLR) of key variables and multiple iterations of the Jarvis Model (described below) for conductance. Model functions for each Jarvis approach were defined based on similar studies done in rice (Xu et al., 2017; Kotani et al., 2017). In this study, PAR was selected as a substitute for net radiation to better reflect plant activity (Campbell et al., 2001). Estimates of ET were calculated using the modeled conductance and compared to field observations to ascertain the impact of conductance on the model output.

The multiple linear regression model (Equation 7) provided estimates for conductance based on photosynthetically active radiation, vapor pressure deficit, and the estimated daily max of conductance based on values estimated from the inversion of the PM AET equation. The MLR model is defined as:

$$g_{c,MLR} = a * PAR + b * VPD + c * T + d \quad \text{(Equation 7)}$$

Where,

- $g_{s,MLR}$ is the modeled conductance value, mm s^{-1}
- T is air temperature, °C
- PAR is photosynthetically active radiation, μmols s^{-1}
- VPD is vapor pressure deficit, kPa
- d is an offset for the model, mm s^{-1}

The standard Jarvis model for conductance (Equation 8) relates key variables linked with canopy conductance to the maximum observed conductance (Jarvis, 1976; Stewart, 1988). The key variables are integrated into the model through functions whose output ranges from zero to one, with each individual function also containing empirically fitted model parameters. For this study, the standard Jarvis model is defined as:

$$g_{c,Jarvis} = g_{c,max} * f(PAR) * f(VPD) \quad \text{(Equation 8)}$$

$$f(PAR) = 1 - e^{(\frac{-PAR}{a1})}$$

$$f(VPD) = 1 - a2 * VPD$$

$$f(T) = 1 - a3 * (25 - T)^2$$

Where,

- a_1, a_2 are model constants
- PAR is photosynthetically active radiation, μmols s^{-1}
- VPD is vapor pressure deficit, kPa
- T is air temperature, °C
- $g_{s,max}$ is the estimated maximum daily conductance for a given day, mm s^{-1}

The second form of the Jarvis equation (Equation 9) utilizes similar functions for the key input variables while also incorporating other field observations, including LAI to scale from leaf to canopy conductance (Xu et al., 2017; Ershadi, 2015). For this study, this form of the Jarvis model (dubbed the Scaled Jarvis model) for conductance is defined as:

$$g_{s,Xu} = g_{s,max} * f(PAR) * f(VPD) * f(T) * LAI_{active} \quad \text{(Equation 9)}$$

$$f(PAR) = 1 - e^{(\frac{-PAR}{a_1})}$$

$$f(VPD) = 1 - a_2 * VPD$$

$$f(T) = 1 - a_3 * (25 - T)^2$$

$$LAI_{active} = \begin{cases} LAI, & LAI \leq 2 \\ \frac{LAI}{2}, & 2 < LAI \leq 4 \\ 2, & 4 < LAI \end{cases}$$

Where,

- a_1, a_2, a_3 are model constants
- PAR is photosynthetically active radiation, μmols s^{-1}
- VPD is vapor pressure deficit, kPa
- T is air temperature, °C
- LAI is leaf area index
- LAI_{active} is the active portion of canopy leaf area index

The final form of the Jarvis equation (Equation 10) utilizes specific inputs from temperature and contains a number of different functions for the typical variables, including PAR, VPD, and temperature, along with the maximum canopy conductance value. Hereafter, this method will be referred to as the "Jarvis-Stewart model".

$$g_{s,Xu} = g_{s,max} * f(PAR) * f(VPD) * f(T) \quad \text{(Equation 10)}$$

$$f(PAR) = \frac{PAR * (PAR_{max} + a_1)}{PAR_{max} * (PAR + a_1)}$$

$$f(VPD) = \left(\left(1 + \left(\frac{VPD}{\sqrt{VPD}}\right)^{a_2}\right) * (1 - a_3)\right) - a_3$$

$$\tau = \frac{T_{max} - T_{opt}}{T_{opt} - T_{min}}$$

$$f(T) = \frac{(T - T_{min}) * (T_{max} - T_{min})^{\tau}}{(T_{opt} - T_{min}) * (T_{max} - T_{opt})^{\tau}}$$

Where,

- a_1, a_2, a_3 are model constants
- PAR is photosynthetically active radiation, μmols s^{-1}
- VPD is vapor pressure deficit, kPa
- T is air temperature, °C
- T_{min} is the minimum seasonal temperature, °C
- T_{opt} is the optimum seasonal temperature where conductance is most active, °C
- T_{max} is the maximum seasonal temperature, °C

Each modeled conductance term was then used as an input into the PM AET model to estimate evapotranspiration at the 30-min time scale for the 2015 growing season. These estimates were compared to eddy covariance observations within the field that did not undergo gap filling via the artificial neural network. Estimation of the parameters for each model was

performed using a nonlinear fit function, which estimated the parameters as functional inputs used in calculating actual evapotranspiration within the PM AET model. To fit the parameters using a nonlinear fit with the PM AET model, eddy covariance estimates were used to simulate actual ET being measured using the PM AET equation.

3. Results

Each model was run using data collected from the 2015 growing season. A total cumulative sum was generated for each model throughout the entire growing season. Each model's predicted outputs were compared with eddy covariance measurements to test their performance using simple linear regression. During this comparison, key inputs for the model were identified as sources of variance between the predicted values and the observations via residual analysis. The PM AET model was also analyzed during both dry (water table below zero) and wet (water table above zero) conditions due to its ability to predict ET at the sub-daily time scale and make use of water table measurements.

3.1 Site and eddy covariance observations

The accumulating GDD values were related to the measured plant parameters to develop a simple, nonlinear equation used to estimate LAI and plant height throughout the season (Figure 1).

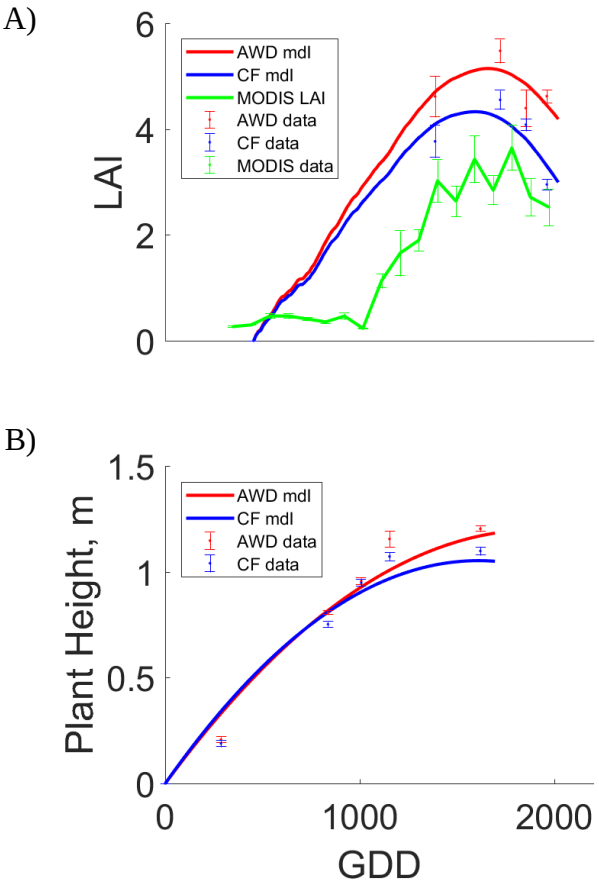

Figure 1. Phenological Development of Rice.

A) Leaf Area Index (LAI) observations collected throughout the 2015 growing season with modeled values (red and blue lines) along with LAI estimated from the MODIS satellite product (green line).

B) Plant height observations collected throughout the 2015 growing season and modeled values (red and blue lines).

The AWD field exhibited higher LAI than the CF during the latter portion of the growing season. The measured plant height within the AWD field was also numerically higher than the CF with significant differences during the latter portion of the growing season as well. The current crop and LAI models assume stable growth during the beginning of the growing season

without inflection, which could cause overestimation of ET during these early parts of the season.

When numerically comparing AWD to the CF treatment, AWD showed greater ET (602 mm) when compared to ET from the CF field (570 mm). The mean evapotranspiration rate for the growing season was 4.4 mm day^{-1} and 4.6 mm day^{-1} for the CF and AWD fields, respectively. Table 2 shows the final estimates of ET for all methods during the 2015 growing season.

Table 2. Summary of ET estimates for each method for 2015 growing season from each respective model applied.

Method	Time Scale	CF Seasonal ET (mm)	AWD Seasonal ET (mm)
PM-AET	Half-Hourly	512	534
PM-FAO56	Daily	610	600
Eddy Covariance	Half-hourly	566	591
Priestley-Taylor	Daily	696	621
BESS	8-Day mean	498	498

To establish a truly conventional flood, the water table depth for the CF field could not fall below the ground level for a significant amount of time. However, the water table depth for the CF field did fall below zero at two points during the growing season for brief (< 1day) periods of time (Figure 2).

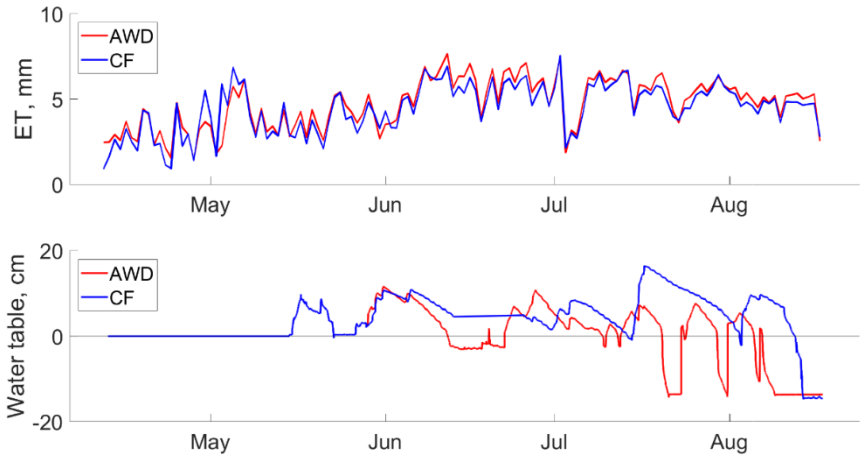

Figure 2. Daily ET estimates for both CF and AWD fields using ANN-gap filled eddy covariance coupled with 30-min water table measurements throughout the 2015 growing season.

The residuals between the AWD and CF field also showed a significant trend as the growing season progressed (Figure 3).

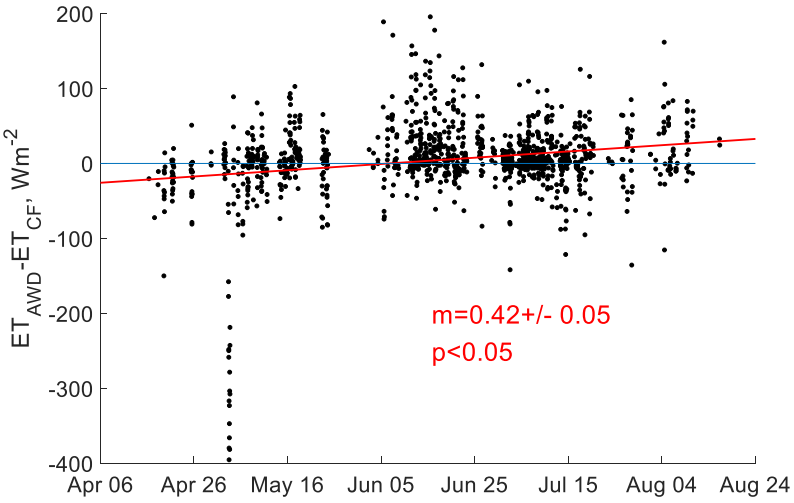

Figure 3. Residuals between the AWD and CF eddy covariance observations (no gap fill) across the 2015 growing season.

To further explore field observations, the season was divided into periods of observation defined by the water table. The periods of observation were set at different periods during the

growing season to eliminate possible bias from the different stages of canopy development. The ET time series from the eddy covariance observations over the course of the season within both fields exhibited possible changing dynamics in the diurnal pattern of ET, which are evident in the smaller periods of observation (Figure 4).

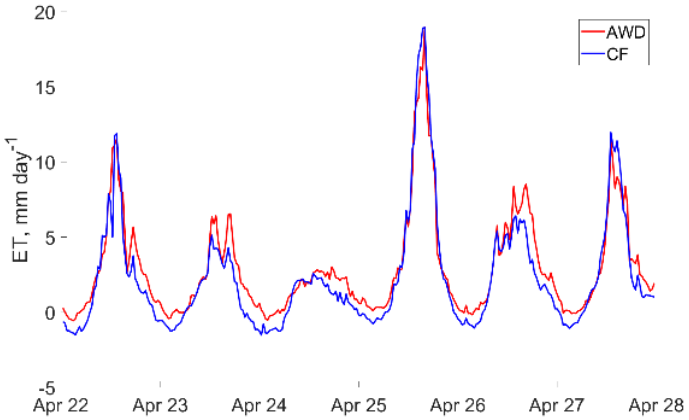

Figure 4. Half hourly eddy covariance observations for ET from both the conventionally flooded (blue) and AWD (red) fields from April 22nd to April 28th for the 2015 growing season.

During the period from April 22nd to April 28th, there was no available data for the water depth within each field, but the surface should not be inundated based on the plant's growth stage and collected field notes. Because it was early in the growing season, we would assume that the state of the canopy was not a factor of change between ET occurring within each field. The comparison of ET during this period showed that the differences were minimal (Figure 5).

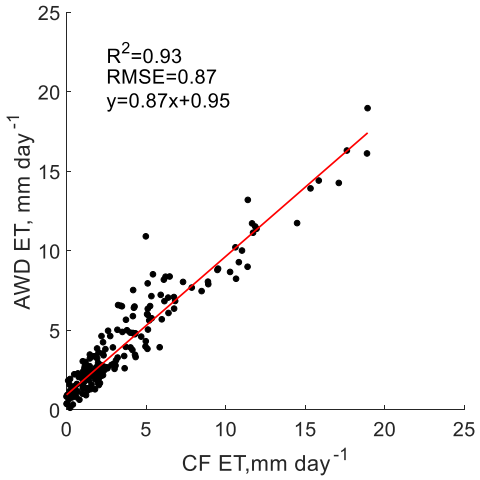

Figure 5. Comparison of half hourly eddy covariance observations in CF and AWD fields from April 22nd to April 28th during the 2015 growing season.

During the period between April 22 and April 28, the slope between AWD and CF was significant ($p<0.05$), meaning that ET measured in the CF field was 13% higher when compared to ET within the AWD field. In order to further investigate these small periods of interest, water table depth was incorporated into the selection process for periods of observation. Water table and soil moisture data were especially important in trying to evaluate the level of drying the field sites were experiencing, specifically within the AWD field (Figure 6). This data makes clear that there is a several day lag between a lowered water table and the corresponding reduction in volumetric water content.

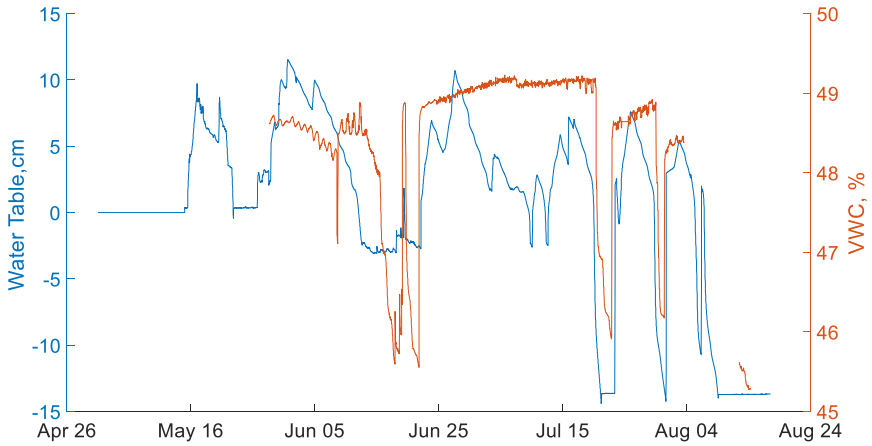

Figure 6. The response of volumetric water content (right axis) to decline in water table (left axis) for the AWD field during the 2015 growing season.

Water table data was collected for the rest of the growing season, beginning in May, so water table depth was added to the analysis for periods occurring after May 1st. The next period of interest occurred between June 5th and June 23rd, where the water table in the AWD field declined significantly for a period of almost 9 full days while the flood remained on the CF field (Figure 7).

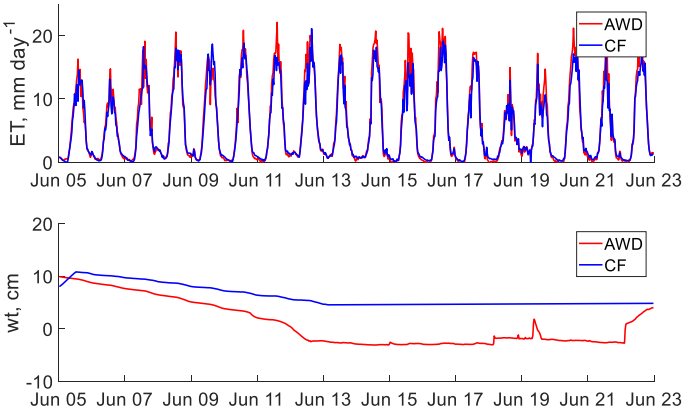

Figure 7. Half hourly ET and water table time series for the conventionally flooded (blue) and AWD (red) fields from June 5th to June 23rd during the 2015 growing season.

This period was most noticeably defined by the declining of the water table in the AWD field while the water table remained stable in the conventionally flooded field. From Figure 7, it appeared that the decline in water table also corresponded to an increase in the amount of evapotranspiration occurring in the AWD field. Despite the decline in the amount of available water for evaporation, the AWD field still showed similar rates of ET to the conventionally flooded field (Figure 8).

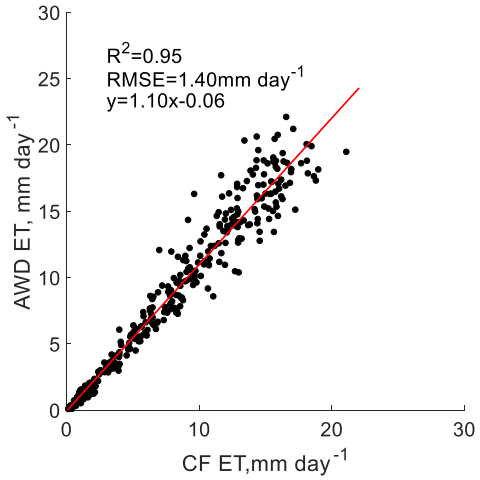

Figure 8. Comparison of half hourly ET in both the CF and AWD fields from June 5 to June 23 during the 2015 growing season.

For the period of June 5 to June 23, the slope between AWD and CF was significant ($p<0.05$), meaning ET during this period was 10% higher in the AWD field compared to the CF field. Using the water table data gathered over this period, the ET observations were divided into two groups of data with each group representing a different water table state for the AWD field (Figure 9).

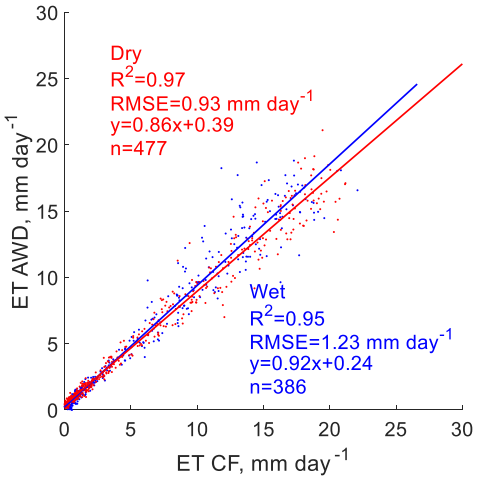

Figure 9. Estimates of ET from EC observations from June 5 to June 23 divided into wet and dry classes based on the water table in the AWD field being above or below zero when compared to the CF field, which had a water table that was above zero over the same period of observation.

The next period was selected between July 18th and July 23rd of 2015 based on similar conditions to the period between June 5th and June 23rd of 2015, where the water table for the AWD field declined below zero for a period of 2 days while the conventionally flooded field remained above ground (Figure 10).

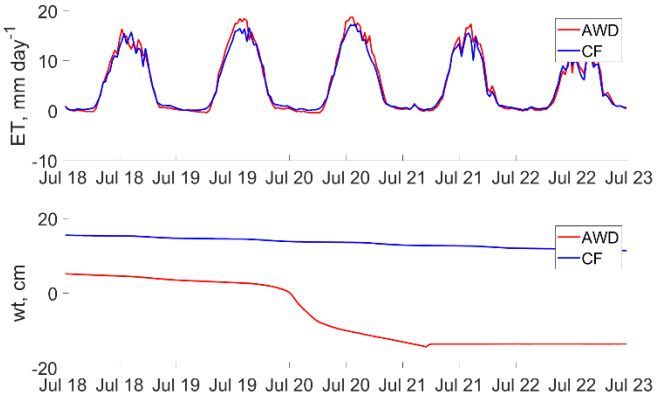

Figure 10. ET and water table time series for the CF (blue) and AWD (red) fields from July 18 to July 23 during the 2015 growing season.

ET data collected over this period were compared similarly to previous periods, with rates being similar between the AWD and CF fields (Figure 11).

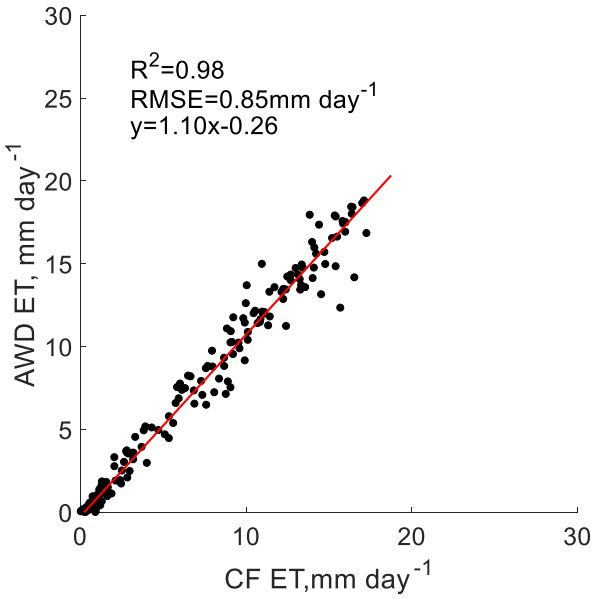

Figure 11. Comparison of ET coming from the CF and AWD fields from July 18 to July 23 during the 2015 growing season.

For the period of July 18 to July 23, the slope between AWD and CF was significant ($p<0.05$), meaning ET during this period was 10% higher in the AWD field compared to the CF field. The data was again separated into wet and dry classes as done previously in order to observe how the shift in water table affected ET being measured at each field (Figure 12).

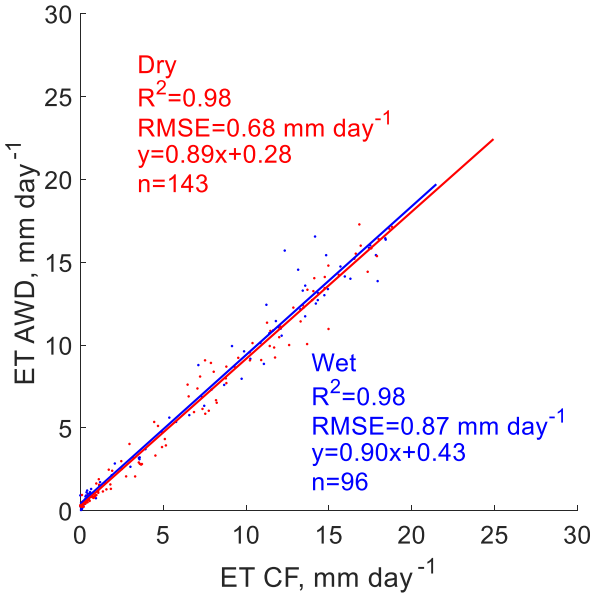

Figure 12. Estimates of ET from EC observations from June 5 to June 23 divided into wet and dry classes based on the water table in the AWD field being above or below zero when compared to the CF field, which had a water table that was above zero over the same period of observation.

3.2 Penman Monteith FAO 56-Crop Coefficient modeling

The applied crop coefficient within the PM FAO56 model is determined over rice grown in different parts of the world. Diversity present in the different varieties of rice as well as unique canopy development patterns, which play a role in ET, could be dampened using a generalized coefficient. To improve the application of the crop coefficient within the PM FAO56 method, the eddy covariance observations were used with the PM FAO 56 equation to develop an estimated crop coefficient from field observations. The estimated crop coefficients for both irrigation regimes and the crop coefficient from PM FAO 56 model varied throughout the season (Figure 13).

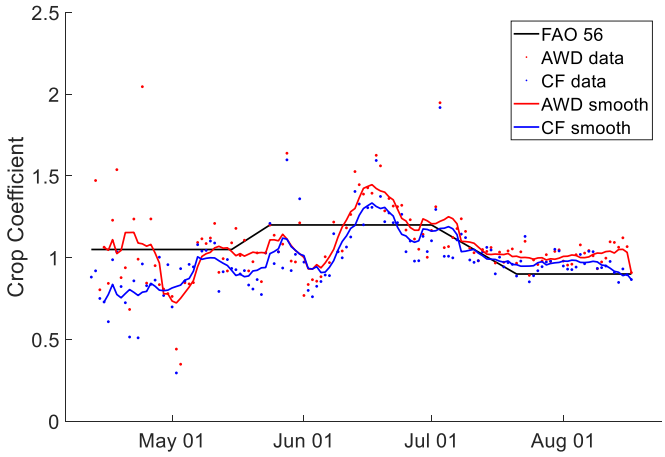

Figure 13. A comparison of the FAO 56 recommended crop coefficient values to crop coefficient calculated from field level observations using the PM FAO 56 equation with eddy covariance observations using data collected from the conventionally flooded field (blue) and AWD field (red). Smoothing uses a 10-day moving window.

Comparing the estimated crop coefficient to the recommended values provided an R^2 value of 0.10 and a RMSE of 0.11 for the 2015 growing season within the conventionally flooded field. Comparing the differences between the estimated crop coefficient and FAO 56 values to measured phenological variables showed that, for the CF field, much of the variance between the two crop coefficients could be explained through plant height and LAI, which are covariates (Table 3).

Table 3. Statistics for the relationship between the estimated crop coefficient using the eddy covariance data and variables linked to rice plant development measured within the conventionally flooded rice field

Phenological Variable (Daily)	R^2	p-value	Slope
LAI	0.25	<0.05	0.0765 ± 0.119
Plant Height	0.29	<0.05	0.3134 ± 0.043
Surface conductance	0.02	<0.05	0.0011 ± 0.003
PAR	0.08	<0.05	0.0004 ± 0.084

The same phenological variables were compared to the differences in crop coefficient for the alternate wetting and drying field, and PAR was able to explain a significant portion of variance between the two crop coefficients. In contrast, plant height and LAI could not significantly explain the variance between estimated and FAO 56 recommended crop coefficient (Table 4).

Table 4. Statistics for the relationship between the estimated crop coefficient using the eddy covariance data and variables linked to rice plant development measured within alternate wetting and drying fields

Phenological Variable (Daily)	R^2	p-value	Slope
LAI	0.01	0.59	0.001 ± 0.019
Plant Height	0.01	0.25	0.091 ± 0.079
Surface conductance	0.01	0.24	-0.002 ± 0.002
PAR	0.20	<0.05	-0.001 ± 0.0002

Analysis showed that each field had different phenologically linked variables which explained the amount of variability between recommended and estimated crop coefficient. LAI and plant height were able to explain almost 30% of the variability in the CF field, while PAR was able to explain 20% within the AWD field.

3.3 PM AET Equation-Conductance modeling

The PM AET model can improve upon the assumptions of the PM FAO 56 by not limiting conductance to a single, constant value (g_s = 14 mm s^{-1}). Conductance is a key term in the PM AET model, whose output is sensitive to changes in conductance throughout the entire growing season. This is evident based on a simple sensitivity analysis showing how a feasible range of conductance values (0 to 100) can affect ET estimates coming from the PM AET model when compared to the eddy covariance observations (Figure 14).

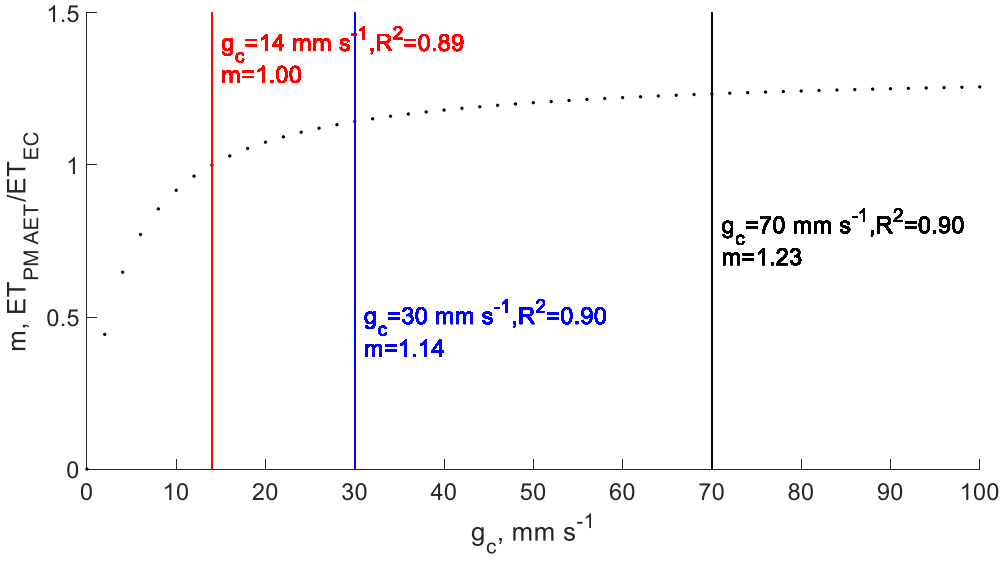

Figure 14. Sensitivity of the PM AET model to changes in conductance when compared to eddy covariance observations over the 2015 growing season for the AWD field.

Based on the analysis in Figure 14, the selected conductance value of 14 mm s^{-1} is a good assumption for the PM FAO56 based on the given slope at that point (m=1). To improve the performance of the PM AET model, canopy conductance was estimated and modeled throughout the 2015 growing season using multiple approaches. The PM AET equation was used to calculated initial estimates of conductance by inverting the equation to solve for conductance using the biometeorological inputs, including field observations of ET from the eddy covariance system. The initial estimates of conductance suffered from the collective error from all the input data, which meant filtering was required to ensure that the conductance estimate was valid while also retaining a suitable amount of data. The data was filtered by removing 30-min data points that corresponded to lower levels of incoming shortwave radiation (<500 Wm^{-2}) and lower levels of observed ET (<5 mm day^{-1}) with the intention of capturing periods where canopy was not limited by solar radiation and active in the exchange of gases through the stomata. The initial

estimates of conductance from the inversion of the PM AET equation showed conductance values ranging between 0 and 30 mm s^{-1} with no clear, recognizable pattern throughout the growing season (Figure 15).

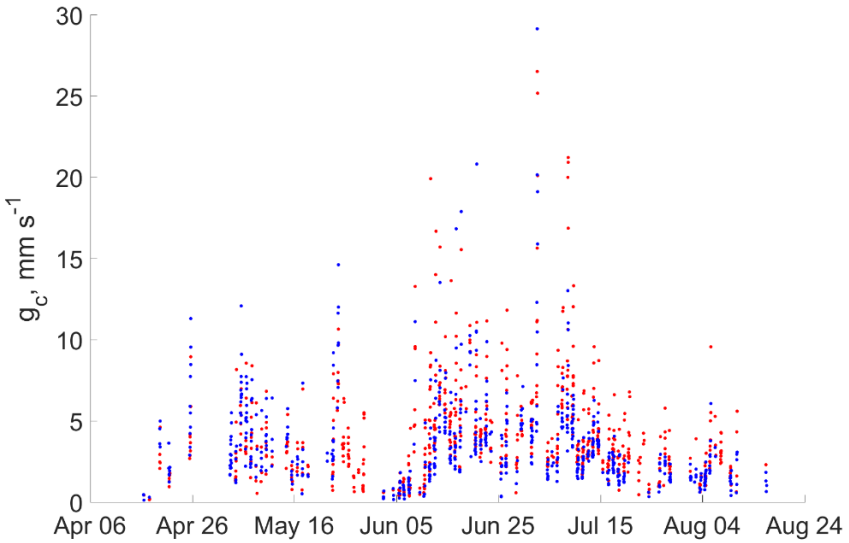

Figure 15. Estimated conductance values from the inversion of the PM AET equation using filters for PAR and input ET for the CF (blue) and AWD (red) fields during the 2015 growing season.

Filtering the data also revealed a suitable estimate for maximum conductance occurring at 30 mm s^{-1}, which was used later in the development of the Jarvis models for conductance. The parameters for the Jarvis models similar to one another in terms of order of magnitude across parameter type (

Table 5). The calculated parameters were dissimilar between each field and irrigation regime. The parameters also did not match well with those found in literature, but this is most likely due to the substitution of net radiation for PAR and the lack of a soil moisture content function.

Table 5. Calculated parameters (a1,a2,a3) for the applied Jarvis conductance models, including values found in literature.

Model	Field	a1	a2	a3
Standard Jarvis	CF	1135.51	0.23	0.0010
	AWD	775.33	0.32	-0.0092
Scaled Jarvis	CF	3183.96	0.18	0.0036
	AWD	2488.66	0.27	0.0012
Jarvis Stewart	CF	682.08	0.59	-0.0615
	AWD	229.79	1.87	-0.1836
*Standard Jarvis-Lit.	AWD	700	-0.046	0.045
*Scaled Jarvis-Lit.	AWD	100.6	0.051	0.0012

* Literature (Xu et al.,2017) models shown in table also incorporated a function for field capacity/soil water content into their models, which would not replicate the models applied in this study.

Despite the differences in parameters, some of the models still performed comparably between irrigation regimes. The performance across all models varied with respect to the modeled actual ET generated from the use of the modeled conductance within the PM AET equation (Table 6).

Table 6. Comparison of PM AET projected ET based on different conductance models to eddy covariance observations for the 2015 growing season with the designated data mask and no gap filling.

Model	Field	R^2	RMSE (Wm^{-2})	p-value
MLR	AWD	0.73	51.3	0
	CF	0.79	60.2	0
Jarvis	AWD	0.84	66	0
	CF	0.66	99.9	0
Jarvis Stewart	AWD	0.29	246	0
	CF	0.84	69.8	0
Scaled Jarvis	AWD	0.84	67.3	0
	CF	0.84	7	0

The Scaled Jarvis model performed well within both the CF and AWD field for the 2015 growing season, so it was selected as the suitable model for conductance to be incorporated into the PM AET model. Features unique to the Scaled Jarvis model include the incorporation of LAI as a factor of influence for the Jarvis equation, which highlighted the differences in the canopy structure throughout the growing season. Performance was comparable between the two fields due to the similarity of other inputs in terms of VPD, temperature, and photosynthetically active radiation.

3.4 ET Model results for the 2015 growing season

All models were applied to the continuously flooded and AWD rice fields to compare their estimates of evapotranspiration. The cumulative evapotranspiration throughout the 2015 growing season for each model showed estimates of ET that were within the same order of magnitude, with model performance changing between fields (Figure 16).

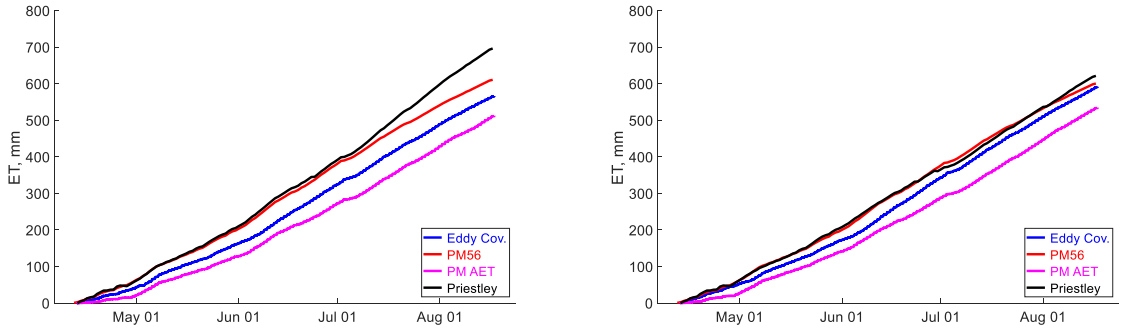

Figure 16. Cumulative ET from each model, including eddy covariance observations, within the conventionally flooded (left) and AWD (right) rice fields for the 2015 growing season (Apr 12 to Aug 18).

The Priestley-Taylor model estimated the highest amount of ET within each irrigation regime. The EC observations also fell within the range of ET presented by the models. The PM

AET model provided the lowest amount of ET within each irrigation regime. Each model was compared to the field observations over the entire 2015 growing season, with varied performance in all models between the CF and AWD fields (Table 7 & Figure 17).

Table 7. Comparison statistics for selected models to the eddy covariance observations for the 2015 growing season in the alternate wetting and drying (AWD) and conventionally flooded (CF) fields

Selected Model	Irrigation	Slope	Intercept	R^2	RMSE (mm day^{-1})
Priestley-Taylor	AWD	0.75	1.10	0.39	1.33
	CF	1.07	0.31	0.64	1.12
PM FAO 56	AWD	0.59	1.66	0.68	0.98
	CF	0.69	1.84	0.77	0.73
PM AET	AWD	1.13	1.13	0.85	2.32
	CF	1.21	-0.64	0.90	1.93

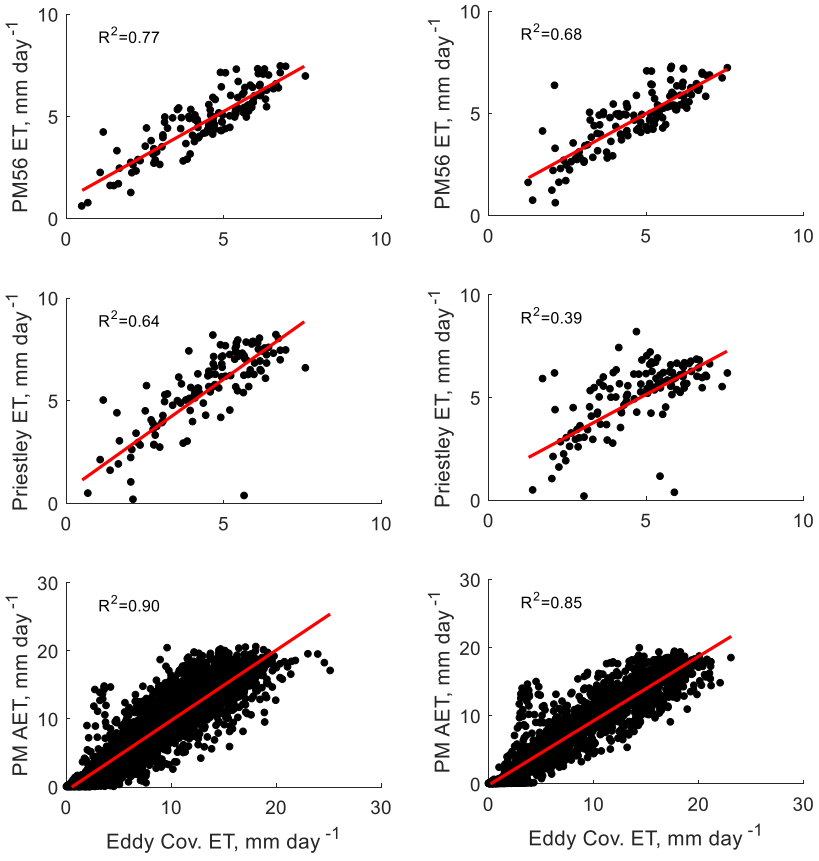

Figure 17. Comparison of model output ET to eddy covariance observations of ET for the 2015 growing season in the conventionally flooded (left) and AWD (right) rice fields.

3.5 Effects of inundation on PM AET model

The PM AET model performance was also evaluated over the selected periods of observation used in examining the eddy covariance observations (

Table 8).

Table 8. Model performance over the selected periods of observation for the 2015 growing season comparing PM AET model using Scaled Jarvis conductance to eddy covariance observations over the same period.

Period			*Field Condition*		*AWD Fit to EC*		*CF Fit to EC*	
Begin	End	Model	AWD	CF	R^2	RMSE (Wm-2)	R^2	RMSE (Wm-2)
28-May	4-Jun	Priestley-Taylor	Wet	Wet	0.82	13.97	0.58	26.08
		PM Pseudo FAO 56	Wet	Wet	0.75	4.59	0.49	6.78
		PM AET	Wet	Wet	0.77	68.45	0.81	62.70
12-Jun	22-Jun	Priestley-Taylor	Dry	Wet	0.88	11.47	0.91	9.91
		PM Pseudo FAO 56	Dry	Wet	0.58	6.14	0.61	6.00
		PM AET	Dry	Wet	0.96	30.25	0.92	43.02
25-Jun	2-Jul	Priestley-Taylor	Wet	Wet	0.71	42.32	0.70	12.38
		PM Pseudo FAO 56	Wet	Wet	0.22	4.96	0.42	4.21
		PM AET	Wet	Wet	0.95	36.94	0.95	42.37
20-Jul	23-Jul	PM AET	Dry	Wet	0.98	25.32	0.97	29.91*
29-Jul	1-Aug	PM AET	Dry	Wet	0.98	24.59	0.98	28.94

The PM AET model showed increased performance as the growing season progressed in both the AWD and CF fields, but performance was similar between the two fields in each given field condition. Because the conductance model did not have an input for soil water content, it is possible that the model did not distinguish differences in soil water content despite changes in temperature and relative humidity within the canopy. The PM AET model also showed no significant change between the AWD and CF ET over the periods of varying inundation, much like the eddy covariance observations.

The Priestley Taylor showed no changes in performance based on the differences in field condition throughout the entire growing season. Because some of the periods of observation were brief (< 2 days), the time scale of the Priestley-Taylor and PM FAO56 models limited meaningful analysis due to the small number of points. The PM FAO 56 model showed no change in performance between differing field conditions across the entire growing season. The poorness of fit during these periods is likely due to the small number of data points incorporated into the analysis.

3.6 Comparison of EC observations to BESS

To derive estimates of ET for our field site using BESS, the selected site was approximately 1 km^2 (Figure 18), which encompassed both the AWD and CF fields. The pixel encompassing the field site does contain images of rice, levees, and small farm roads, which could alter inputs such as LAI in some small fraction.

Figure 18. Image of field site using MODIS for inputs into BESS (taken from MODIS & Google Maps).

Because BESS estimates ET from the establishment of MODIS, we could put the 2015 ET estimates from BESS into context for the previous 15 years (Figure 19):

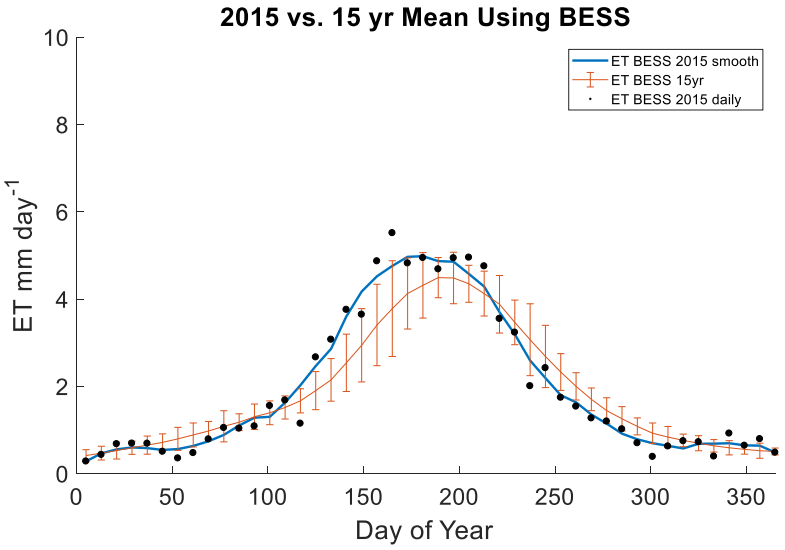

Figure 19. Comparison of ET from BESS in 2015 to the 15 year mean of ET estimated using BESS.

According to BESS, ET from the 2015 growing season seems to have higher amounts of ET occurring earlier in the season when compared to the 15-year mean. This could be a product of an earlier planting date that occurred that year. BESS also provided estimates of ET well within the order of magnitude of the field observations for both irrigation regimes (Figure 20).

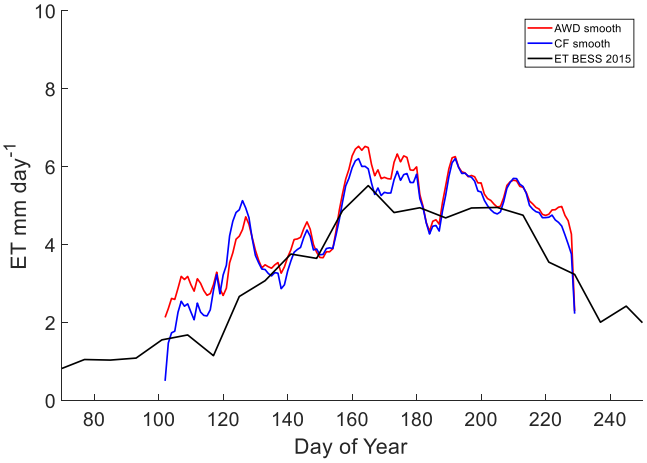

Figure 20. Comparison of BESS ET to ET observed from eddy covariance stations for the 2015 growing season.

Cumulative estimates of ET showed BESS underpredicting seasonal ET as well (Table 2). The consistent underestimation was also valid when comparing the calculated 8-day mean of the eddy covariance observations to their BESS counterparts (Figure 21).

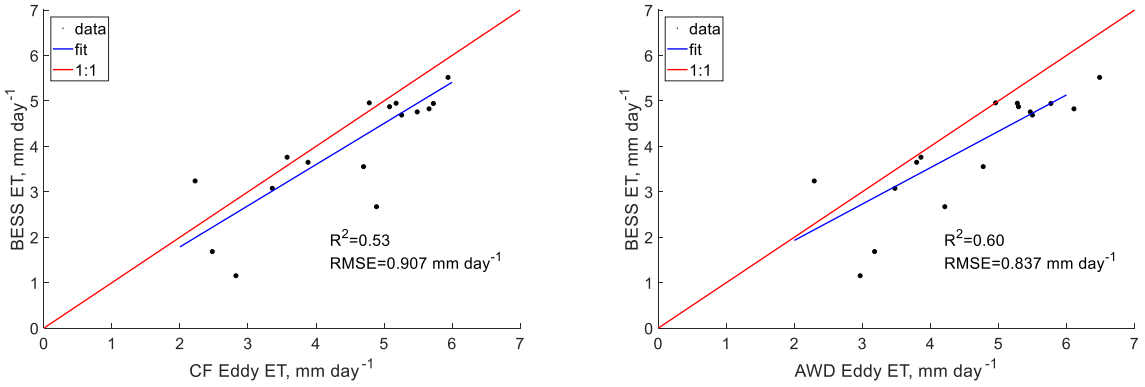

Figure 21. Comparison of 8-day means between BESS and eddy covariance observations for the 2015 growing season.

When comparing LAI estimated over this time using the MODIS product to LAI measured directly from the field, the difference in values showed no strong correlation to the residuals between ET calculated from BESS and ET observed within the field. However, because LAI is an important component in accounting for transpiration occurring within the field, it should not be assumed that LAI has no significant effect on ET. It is possible that with better modeling of LAI based on field measurements taken on the ground, the model's performance could be improved.

4. Discussion

4.1 Effects of irrigation regimes on ET

Based on the field observations, the AWD and CF fields produced the very similar ET for the 2015 growing season. Observational periods showed significant differences in ET within areas of dry down. However, the AWD field experience higher amounts of ET during two of the observational periods associated with the water table declining below zero, which does not agree the initial hypothesis involving available water and evaporation. During the early period of the growing season, both fields had similar water levels and LAI, which would suggest that ET between the two fields should be similar. During the latter portion of the season, as the canopy progressed rapidly in development, it is possible that transpiration accounted for a majority of the amount of ET occurring during this period, which would also explain why the rate of ET decline as the water table changed dramatically within the AWD field. However, the AWD field still showed higher amounts of ET during the latter portion of the growing season when compared to the CF field while the water table within the AWD field fell below zero at three points for extended periods of time.

Because ET was not significantly different between the CF and AWD fields, it can be assumed that the amount of stomatal activity between the two fields was similar despite the changing water table. If the rice plants could stay active and produce comparable yields despite the declining water table, AWD could be a viable solution for water savings within this field site. As mentioned earlier, water savings for AWD are a direct result of the producer's ability to take advantage of rains occurring during the growing season while the ground on the field remains dry. Any amount of rain captured within the field offsets the amount of water the farmer will be required to pump to keep the plants alive and active.

4.2 Model performance and selection

Based on the analysis of each model across the growing season, the PM AET model provided the best estimate of ET across the entire growing season in all field conditions and irrigation regimes. This was likely due to the increased complexity of the model, which used inputs related to both the biological and meteorological conditions of the canopy to accurately estimate ET. Because of its ability to produce accurate estimates of ET using well defined and supported mechanics, the PM AET model should be used in future efforts to monitor ET in lieu of the Priestley-Taylor or PM FAO56 models.

To improve the performance of the PM FAO56 model, a proper reference site must be used to calculate reference ET. Having a well-maintained FAO 56 alfalfa site is important in gaining an accurate estimate of both daily ET and crop coefficient. Drivers for the crop coefficient should also be more evident when using proper reference ET and field observations. Eddy covariance and lysimeters have served as suitable estimates of crop evapotranspiration, but correct reference ET is critical in estimating crop coefficient utilizing a suitable alfalfa site (Anderson et al., 2017; Tiyagi et al., 2000). The PM FAO56 crop coefficients showed similar patterns to the estimate of crop coefficient using eddy covariance observations. Biometeorological variables measured within the field (LAI, PAR, etc.) was also able to explain some of the variance between the estimates and recommended values. Incorporating these variables into a localized crop coefficient model could continue to improve the PM FAO56 method within each field site.

Within both iterations of the Penman Monteith equation, there is a critical assumption that the ground heat flux represents a constant fraction of net radiation throughout the entire season. However, the amount of ground heat flux occurring within the field is a function of water

table height and temperature as well. As the amount of available water decreases, there is a smaller buffer for heat flux, which would be reflected in the shifting of available energy (RN-G) throughout the day. It is also valid to say that in cases where the water table declined below the surface, the AWD field should have exhibited higher amounts of sensible heat flux and longwave net radiation (meaning decreased net radiation), which have been demonstrated in fields using AWD (Alberto et al., 2011). Specifically, in the study by Alberto, they observed net radiation as a key driver in ET, which is also consistent with the findings from the PM models in our field site. They also confirmed that the AWD rice as having lower amounts of ponding and lower LAI, leading to lower ET. In contrast, the drought stress observed within the fields led to lower yields, which was not the case in our study.

The BESS product performed well given that the amount of input information was low, yet it was still able to generate a valid estimate of ET. Incorporation of field observations directly to BESS could help calibrate the product over rice and improve performance. BESS has the advantage over other models in its applied scope and use of legacy data.

4.3 Modeling canopy conductance

The Scaled Jarvis model provided the best estimate for conductance within both irrigation regimes and was deemed suitable for adaptation into AR rice. Conductance was shown to be critical in the determination of actual ET from the PM AET when compared to the eddy covariance observations.

5. Conclusions

The model estimates were comparable to the eddy covariance observations in terms of magnitude, and the eddy covariance values fell within the range of ET predicted by the models.

The measured amounts of ET from eddy covariance for the AWD and CF fields were 591 mm and 566 mm, respectively. The eddy covariance estimates were similar to one another throughout the growing season, but they were also shown to be significantly different under smaller observational periods with differing levels of inundation. Yields measured between the fields were also statistically insignificant, but LAI was higher in the AWD field compared to the CF field. The experiment showed that despite a declining water table, stomatal activity displayed in the canopies via ET was undisturbed. Because AWD is associated with fear of possible drought stress, this study shows that a declination of the water table for a small period of time will not necessarily disrupt plant activity.

The PM AET model performed the best in terms of estimating ET. The performance of the PM AET model was dependent on the incorporated conductance models, which were different for each field. The scaled Jarvis conductance model yielded the best estimates of ET for the AWD field while the Jarvis-Stewart model yielded the best estimates of ET for the CF field during the 2015 growing season. The primary differences between the conductance model inputs included the inclusion of LAI as a factor of change for the Scaled Jarvis model.

The differences in the AWD field and the CF field were minimal in terms of ET. It is possible that due to a higher amount of plant surface area and density, as seen through LAI measurements and yield data, the AWD field could have produced higher amounts of ET due to higher amount of transpiration occurring. It is also possible that the plants were not limited in conductance of water between the canopy and the atmosphere due to the depth of the roots and the availability of water just underneath the ground.

6. References

Alberto, M.C.R., Wassmann, R., Hirano, T., Miyata, A., Hatano, R., Kumar, A., Padre, A. and Amante, M., 2011. Comparisons of energy balance and evapotranspiration between flooded and aerobic rice fields in the Philippines. *Agricultural Water Management*, Vol. 98(9), pp.1417-1430.

Allen, R.G. and Pruitt, W.O., 1991. FAO-24 reference evapotranspiration factors. *Journal of Irrigation and Drainage Engineering*, Vol.117 (5), pp.758-773.

Allen, Richard G., et al. 1998. "Crop evapotranspiration-Guidelines for computing crop water requirements-FAO Irrigation and drainage paper 56". *FAO, Rome*300.9: D05109.

Anders, M.M., Watkins, K.B., Nalley, L.L., Siebenmorgen, T.J. and Brye, K.R., 2012. Growing rice with less water. *Rice Research Studies–2011. Series, 600*, pp.188-194.

Anderson, D.E., Verma, S.B. and Rosenberg, N.J., 1984. Eddy correlation measurements of CO_2, latent heat, and sensible heat fluxes over a crop surface. *Boundary-Layer Meteorology*, Vol. 29(3), pp.263-272.

Anderson, R.G., Alfieri, J.G., Tirado-Corbalá, R., Gartung, J., McKee, L.G., Prueger, J.H., Wang, D., Ayars, J.E. and Kustas, W.P., 2017. Assessing FAO-56 dual crop coefficients using eddy covariance flux partitioning. *Agricultural Water Management*, *179*, pp.92-102.

ANRC, 2014. Arkansas Water Plan Update 2014. Available at: http://arkansaswaterplan.org/plan/ArkansasWaterPlan/2014AWPWaterPlan/AWPFinalExecutiveSumm.pdf#page=15 [Accessed on May 16, 2016].

ANRC, 2015. Arkansas Groundwater Protection and Management Report for 2015. Available at: https://static.ark.org/eeuploads/anrc/FINAL_DRAFT_groundwater_rpt_2015-2016.pdf [Accessed on May 16, 2016].

AR Rice. 2011. Arkansas Rice Facts. *Arkansas Rice Federation*. http://www.arkansasricefarmers.org/arkansas-rice-facts/ (Cached).

Baldocchi, Dennis, Riccardo Valentini, Steve Running, Walt Oeche L, and Roger Dahlman. 1996. "Strategies for measuring and modelling carbon dioxide and water vapour fluxes over terrestrial ecosystems." *Global Change Biology*, Vol.2 (3) pp 159-168.

Belder, P., Bouman, B.A.M. and Spiertz, J.H.J., 2007. Exploring options for water savings in lowland rice using a modelling approach. *Agricultural Systems*, *92*(1), pp.91-114.

Campbell, C.S., Heilman, J.L., McInnes, K.J., Wilson, L.T., Medley, J.C., Wu, G. and Cobos, D.R., 2001. Seasonal variation in radiation use efficiency of irrigated rice. *Agricultural and Forest Meteorology*, *110*(1), pp.45-54.

Carrijo, D.R., Lundy, M.E. and Linquist, B.A., 2017. Rice yields and water use under alternate wetting and drying irrigation: A meta-analysis. *Field Crops Research*, *203*, pp.173-180.

Doorenbos, J. and Kassam, A. H. 1979. *Yield response to water.* FAO Irrig. and Drain. Paper No. 33, FAO, Rome, Italy. 193 pp.

Doorenbos, J. and Pruitt, W. O., 1977. Crop water requirements. *Irrigation and Drainage Paper No. 24*, (rev.) FAO, Rome, Italy. 144 p.

Ershadi, A., McCabe, M.F., Evans, J.P. and Wood, E.F., 2015. Impact of model structure and parameterization on Penman–Monteith type evaporation models. *Journal of Hydrology*, *525*, pp.521-535.

Foken, T., Wimmer, F., Mauder, M., Thomas, C. and Liebethal, C., 2006. Some aspects of the energy balance closure problem. *Atmospheric Chemistry and Physics*, *6*(12), pp.4395-4402.

Henry, C.G., Hirsh, S.L., Anders, M.M., Vories, E.D., Reba, M.L., Watkins, K.B. and Hardke, J.T., 2016. Annual irrigation water use for Arkansas rice production. *Journal of Irrigation and Drainage Engineering*, *142*(11), p.05016006.

Jarvis, P.G., 1976. The interpretation of the variations in leaf water potential and stomatal conductance found in canopies in the field. Philosophical Transactions of the Royal Society of London, Series B, 593–610.

Jiang, C. and Ryu, Y., 2016. Multi-scale evaluation of global gross primary productivity and evapotranspiration products derived from Breathing Earth System Simulator (BESS). *Remote Sensing of Environment*, *186*, pp.528-547.

Kustas, W.P. and Daughtry, C.S., 1990. "Estimation of the soil heat flux/net radiation ratio from spectral data." *Agricultural and Forest Meteorology*, Vol.49 (3), pp.205-223.

Lamine, D., Bodian, A. and Diallo, D., 2015. Use of atmometers to estimate reference evapotranspiration in Arkansas. *African Journal of Agricultural Research*, Vol. 10(48), pp.4376-4383.

Lampayan, R.M., Rejesus, R.M., Singleton, G.R. and Bouman, B.A., 2015. Adoption and economics of alternate wetting and drying water management for irrigated lowland rice. *Field Crops Research*, *170*, pp.95-108.

Linquist, B.A., Anders, M.M., Adviento-Borbe, M.A.A., Chaney, R.L., Nalley, L.L., Da Rosa, E.F. and Kessel, C. 2015. "Reducing greenhouse gas emissions, water use, and grain arsenic levels in rice systems." *Global Change Biology*, Vol.21 (1), pp.407-417.

Mohan, S., 1991. "Intercomparison of evapotranspiration estimates." *Hydrological Sciences Journal*, Vol. 36(5) pp. 447-460.

Monteith, J.L., 1965. "Evaporation and environment." *State and Movement of Water in Living Organisms, 19th Symposium of the Society for Experimental Biology*. Cambridge University Press, Cambridge, pp. 205-234.

Monteith, J.L., 1981. Evaporation and surface temperature. *Quarterly Journal of the Royal Meteorological Society*, Vol.107 (451), pp.1-27.

Olk, D.C. et al. 2009. "Crop Nitrogen Uptake and Soil Phenols Accumulation under Continuous Rice Cropping in Arkansas." *Soil Science Society of America Journal*, Vol. 73(3), pp.952.

Pan, J., Liu, Y., Zhong, X., Lampayan, R.M., Singleton, G.R., Huang, N., Liang, K., Peng, B. and Tian, K., 2017. Grain yield, water productivity and nitrogen use efficiency of rice under different water management and fertilizer-N inputs in South China. *Agricultural Water Management*, *184*, pp.191-200.

Papale, D. and Valentini, R., 2003. A new assessment of European forests carbon exchanges by eddy fluxes and artificial neural network spatialization. *Global Change Biology*, *9*(4), pp.525-535.

Penman, H.L., 1948, April. Natural evaporation from open water, bare soil and grass. *In Proceedings of the Royal Society of London: Mathematical, Physical and Engineering Sciences* Vol. 193, No. 1032, pp. 120-145.

Penman, Howard Latimer. 1948. "Natural evaporation from open water, bare soil and grass." In *Proceedings of the Royal Society of London A: Mathematical, Physical and Engineering Sciences*, Vol. 193, no. 1032, pp. 120-145.

Priestley, C.H.B. and Taylor, R.J., 1972. On the assessment of surface heat flux and evaporation using large-scale parameters. *Monthly Weather Review*, Vol.100 (2), pp.81-92.

Pruitt, W. O. 1986. "Traditional methods 'Evapotranspiration research priorities for the next decade'." *ASAE* Paper No. 86-2629. 23 p.

Reba, M.L., Daniels, M., Chen, Y., Sharpley, A., Bouldin, J., Teague, T.G., Daniel, P. and Henry, C.G., 2013. A statewide network for monitoring agricultural water quality and water quantity in Arkansas. *Journal of Soil and Water Conservation*, *68*(2), pp.45A-49A.

Scott, H.D., Ferguson, J.A., Hanson, L., Fugitt, T. and Smith, E. 1998. "Agricultural water management in the Mississippi Delta region of Arkansas." In *Res. Bull. 959*, Arkansas Agricultural Experiment Station Fayetteville. *98*.

Smith, M.C., Massey, J.H., Branson, J., Epting, J.W., Pennington, D., Tacker, P.L., Thomas, J., Vories, E.D. and Wilson, C., 2007. Water use estimates for various rice production systems in Mississippi and Arkansas. *Irrigation Science*, Vol. *25*(2), pp.141-147.

Snyder, R. L., Lanini, B. J., Shaw, D. A., and Pruitt, W. O. 1989a. Using reference evapotranspiration (ETo) and crop coefficients to estimate crop evapotranspiration (ETc) for agronomic crops, grasses, and vegetable crops. Cooperative Extension, Univ. California, Berkeley, CA, Leaflet No. 21427, 12 p.

Snyder, R. L., Lanini, B. J., Shaw, D. A., and Pruitt, W. O. 1989b. Using reference evapotranspiration (ETo) and crop coefficients to estimate crop evapotranspiration (ETc) for trees and vines. Cooperative Extension, Univ. California, Berkeley, CA, Leaflet No. 21428, 8 p.

Stewart, J.B., 1988. Modeling surface conductance of pine forest. Agricultural and Forest Meteorology 43, 19–35.

Stewart, R.B. and Rouse, W.R., 1977. Substantiation of the Priestley and Taylor parameter α= 1.26 for potential evaporation in high latitudes. *Journal of Applied Meteorology*, *16*(6), pp.649-650.

Timm, A.U., Roberti, D.R., Streck, N.A., Gustavo G. de Gonçalves, L., Acevedo, O.C., Moraes, O.L., Moreira, V.S., Degrazia, G.A., Ferlan, M. and Toll, D.L., 2014. Energy partitioning and evapotranspiration over a rice paddy in Southern Brazil. *Journal of Hydrometeorology*, Vol.15 (5), pp.1975-1988.

Tyagi, N.K., Sharma, D.K. and Luthra, S.K., 2000. Determination of evapotranspiration and crop coefficients of rice and sunflower with lysimeter. *Agricultural Water Management*, *45*(1), pp.41-54.

Walter, I.A., Allen, R.G., Elliott, R., Jensen, M.E., Itenfisu, D., Mecham, B., Howell, T.A., Snyder, R., Brown, P., Echings, S. and Spofford, T., 2000. ASCE's standardized reference evapotranspiration equation. In*Proc. of the Watershed Management 2000 Conference, June*.

Watkins, K.B., Hristovska, T., Mazzanti, R., Wilson Jr, C.E. and Schmidt, L., 2014. Measurement of technical, allocative, economic, and scale efficiency of rice production in Arkansas using data envelopment analysis. *Journal of Agricultural and Applied Economics*, Vol. 46 (1), p.89.

Wilson Jr, C.E., Runsick, S.K. and Mazzanti, R., 2007. Trends in Arkansas rice production. *BR Wells rice research studies*, pp.11-20.

Wright J. L. 1981. Crop coefficients for estimates of daily crop evapotranspiration. *Irrig. Scheduling for Water and Energy Conservation in the 80s*, ASAE, Dec. 1981.

Wright, J. L. 1982. New Evapotranspiration Crop Coefficients. *Journal of Irrigation and Drainage Div.*, ASCE, 108: 57-74.

Yang, S., Logan, J. and Coffey, D.L., 1995. Mathematical formulae for calculating the base temperature for growing degree days. *Agricultural and Forest Meteorology*, *74*(1-2), pp.61-74.